Irradiations with 24 GeV/c protons of Lead Tungstate, LYSO and Cerium Fluoride crystals

A comparison to CMS running conditions

ETH Institute for Particle Physics

ETHZ-IPP-2014-02
December 18th, 2014

Irradiations with 24 GeV/c protons of Lead Tungstate, LYSO and Cerium Fluoride crystals: a comparison to CMS running conditions

F. Nessi-Tedaldi, M. Quittnat

Institute for Particle Physics, ETH Zurich, 8093 Zurich, Switzerland

Abstract

This note summarizes the fluences and energy spectra present in the irradiation of long Lead Tungstate, LYSO and Cerium Fluoride crystals for different particle types and compares them to fluences and energy spectra expected in the CMS endcaps (EE) at the High-Luminosity LHC (HL-LHC). The derived scaling factors might allow the usage of a measured damage amplitude for anticipating the CMS EE performance evolution.

1 Introduction

This note aims to answer the questions asked by the EC reviewers group that scrutinizes the different options for the EE Phase II upgrade of CMS. It summarizes FLUKA results obtained for 24 GeV/c proton irradiations of long crystal samples performed at the PS and compares them to the CMS particle fluences and doses expected in situ, during pp collisions. The information collected herein should allow to easily determine the scaling between existing irradiation results and the exposure the calorimeter will experience during CMS running.

2 Overview of results about hadron effects in lead tungstate

Extensive studies performed during R& D for the CMS ECAL and for other experiments have shown that ionizing radiation reduces light transmission in lead tungstate, through the formation of color centers: it has been generally observed that this kind of damage reaches an equilibrium at a level proportional (not necessarily linearly) to the dose rate. In addition, however, the hadron fluences cumulated during LHC running are expected to induce an additional, hadron-specific change of light transmission.

Studies of hadron damage in lead tungstate have been summarized in [1] and have been studied over more than 2 orders of magnitude in fluence, up to 5×10^{13} p/cm^2, that corresponds to a pseudorapidity $\eta \simeq 2.8$ for $\int \mathcal{L}dt = 500$ fb^{-1} in 14 TeV pp collision energies, and for fluxes ranging from 5×10^{11} p/cm^2/h to 1×10^{13} p/cm^2/h, with no rate dependence seen. It has been established that hadrons induce, similarly to ionizing radiation, a reduction of crystal light transmission which is cumulative [2] while no indication is observed of a hadron-specific change to the scintillation emission [3], a feature which is crucial for the ability to monitor also hadron-induced changes through light injection. Furthermore, it has been experimentally verified that the damage due to the 24 GeV/c protons used in most tests and to 290 MeV/c charged pions, which are more representative for the particle spectrum in the EE, scales in the same way as star densities from FLUKA simulations [4]. This is consistent with the understanding gained in these studies, that hadron damage in lead tungstate is due to disorder caused by an intense local energy deposition from heavy fragments.

The Rayleigh-scattering behavior of light diffused inside hadron-irradiated crystals confirms this understanding, in that it is polarized and exhibits a λ^{-4} dependence. Such a mechanism of damage was expected to be absent in crystals with elements below Z=71 [5], and this has recently been confirmed by a hadron damage test on Cerium Fluoride [6]. The damage is usually quantified through the longitudinal induced absorption coefficient for a given wavelength λ, which is defined as

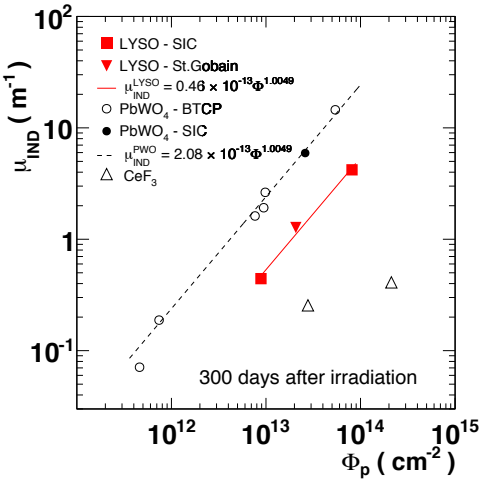

(a) Induced absorption coefficient versus proton fluence for lead tungstate crystals of different length and origin, for LYSO and for CeF_3, from [7].

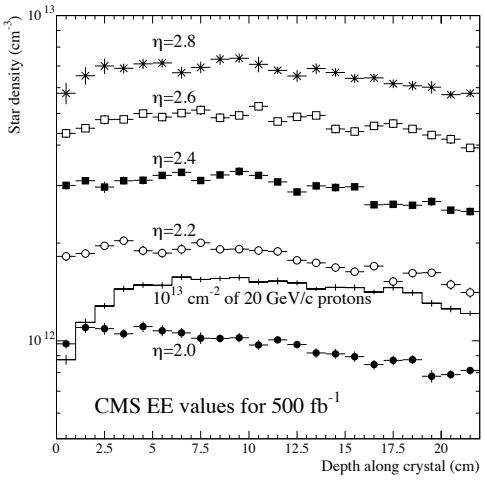

(b) Star densities at different η in the EE for 500 fb^{-1} at 14 TeV and for a single crystal irradiated with 10^{13} p/cm^{-2} at 20 GeV/c, from [2].

Figure 1: Main results concerning Lead Tungstate, LYSO and CeF_3. See text for details.

$$\mu_{IND}^{LT}(\lambda) = \frac{1}{\ell} \times \ln \frac{LT_0}{LT} \tag{1}$$

where LT_0 (LT) is the longitudinal transmission value measured before (after) irradiation through the length ℓ of the crystal, and analogously for transverse transmission (TT). In all the measurements that enter this note, $\mu_{IND}^{LT}(420\text{ nm})$ has been used, since this wavelength is the most relevant one as it corresponds to the maximum of scintillation emission. Herein, the short form μ_{IND}^{LT} is also used for the same quantity.

The cumulative behavior of μ_{IND}^{LT} with fluence can be appreciated in Fig. 1(a), and the star densities from FLUKA simulations relevant for the parametrization presented herein are found in Fig. 1(b) from [2]. Based on the studies mentioned above, the evolution of light transmission due to hadrons that might have to be expected in the CMS ECAL has been extracted [8, 9]. The PS irradiation fluence corresponding to a given η-bin in CMS can easily be read off Fig. 1(b).

3 Particle fluences at the PS and during CMS running

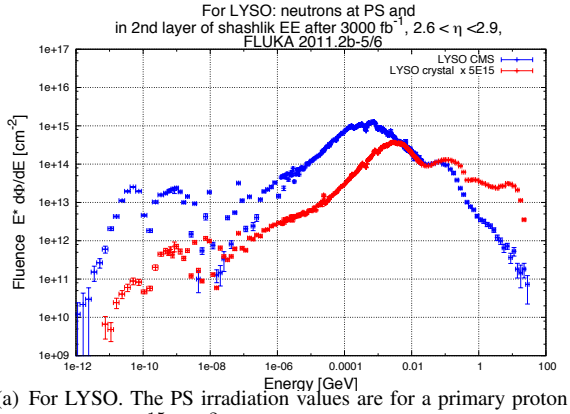

(a) For LYSO. The PS irradiation values are for a primary proton fluence of $5 \times 10^{15}\text{cm}^{-2}$.

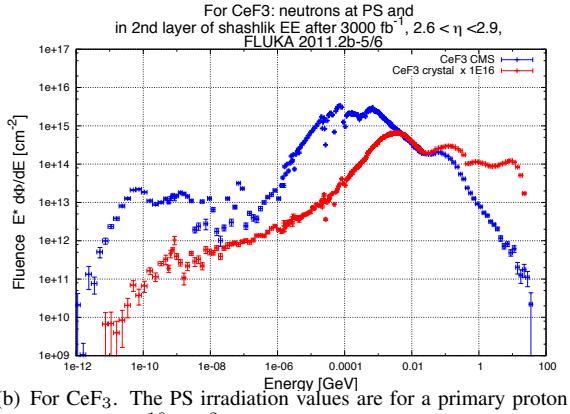

(b) For CeF_3. The PS irradiation values are for a primary proton fluence of $1 \times 10^{16}\text{cm}^{-2}$.

Figure 2: Neutron fluence spectra in the second layer of a Shashlik CMS EE for 3000 fb^{-1} in the pseudorapidity range $2.6 <| \eta |< 2.9$, and in a long crystal irradiated with 24 GeV/c protons at the CERN PS.

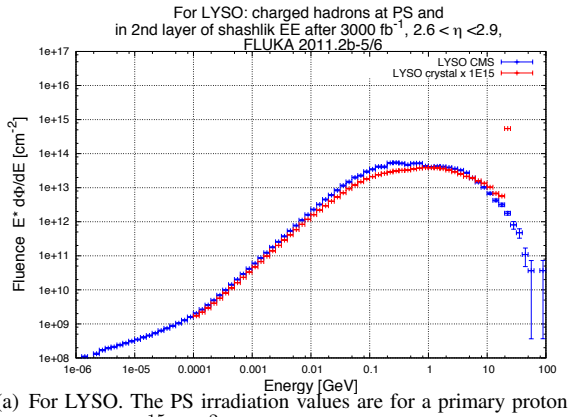

(a) For LYSO. The PS irradiation values are for a primary proton fluence of $1 \times 10^{15}\text{cm}^{-2}$.

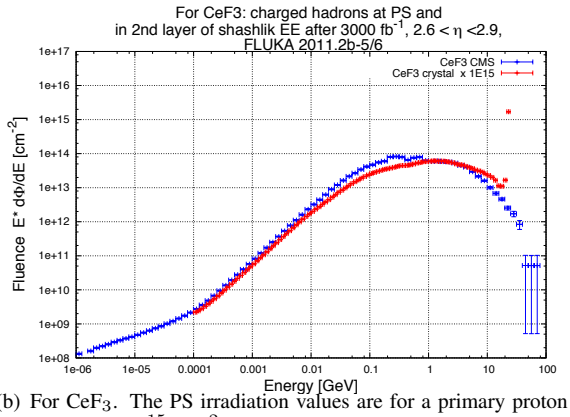

(b) For CeF_3. The PS irradiation values are for a primary proton fluence of $1 \times 10^{15}\text{cm}^{-2}$.

Figure 3: Charged hadron fluence spectra in the second layer of a Shashlik CMS EE for 3000 fb^{-1} in the range $2.6 <| \eta |< 2.9$, and in a long crystal irradiated with 24 GeV/c protons at the CERN PS.

Spectra of particle fluences have been studied for an upgraded CMS detector for the HL-LHC, with an EE calorimeter implemented as a sampling geometry. The details of this study are found in Ref. [10]. The present summary only intends to give practical means of relating PS proton-irradiation results on crystal damage to the CMS running conditions for the HL-LHC. The proton irradiations have yielded results for 10 cm long LYSO [7] and 14.1 cm

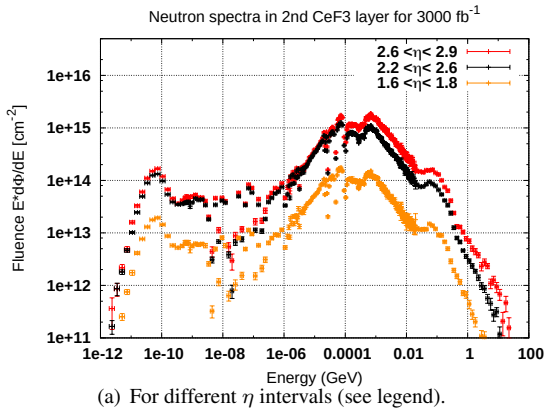

(a) For different η intervals (see legend).

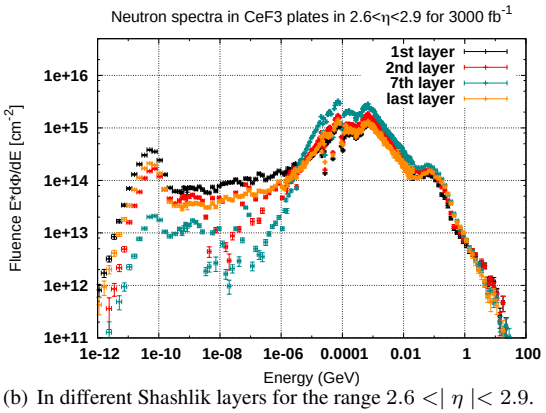

(b) In different Shashlik layers for the range $2.6 <| \eta |< 2.9$.

Figure 4: For CeF_3, neutron spectra in CMS for 3000 fb^{-1}.

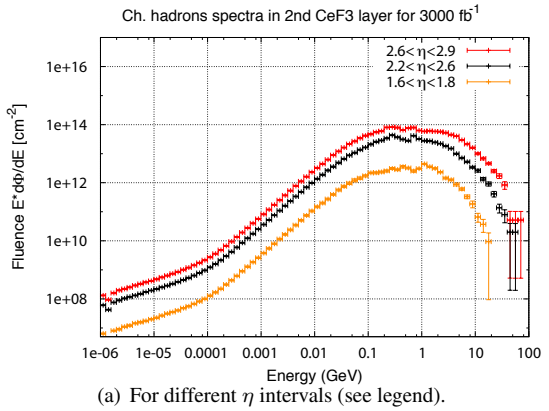

(a) For different η intervals (see legend).

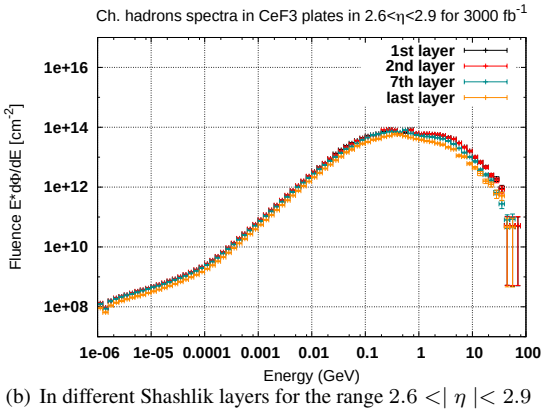

(b) In different Shashlik layers for the range $2.6 <| \eta |< 2.9$

Figure 5: For CeF_3, charged hadron spectra in CMS for 3000 fb^{-1}.

long CeF_3[6] samples. The length being quite important, since it was chosen to be sufficient to allow a hadronic shower to develop.

Example fluence spectra are given in Fig. 2 for neutrons and in Fig. 3 for charged hadrons in a Shashlik CMS EE compared to the spectrum caused by protons in the corresponding crystal, for the specific irradiations described in Refs. [7, 6]. The values in CMS are given for the second EE scintillator layer as this is the layer with the highest absorbed dose rate [10].

For neutrons, the relative amount of thermal and epithermal neutrons is lower in the PS irradiation, due to the smaller amount of surrounding materials compared to the CMS environment. One can crudely distinguish four energy intervals wherein the shape of the spectrum is quite similar between CMS and the p-irradiation, up to a multiplicative factor. For this reason, the comparison of fluences in energy intervals up to 0.5 MeV, 20 MeV, 200 MeV is discussed below. For charged hadrons, the shape of the spectra between CMS EE and PS are quite similar and a single scaling factor might well be applicable.

Table 1: Fluence values in LYSO for a 24 GeV/c proton irradiation at the CERN PS and in the 2nd LYSO layer of a Shashlik CMS EE after 3000 fb^{-1} of collected data.

Energy interval	neutrons PS [$cm^{-2}p^{-1}$]	ch. had. PS [$cm^{-2}p^{-1}$]	CMS n η: 2.6-2.9 [cm^{-2}]	CMS n η: 2.2-2.6 [cm^{-2}]	CMS ch. had. η: 2.6-2.9 [cm^{-2}]	CMS ch.had. η: 2.2-2.6 [cm^{-2}]
E < 0.5 MeV	3.11E-02	5.66E-06	3.76E+15	2.64E+15	1.35E+10	5.96E+09
0.5 MeV<E< 20 MeV	6.23E-02	6.83E-04	1.96E+15	1.11E+15	1.27E+11	5.58E+10
20 MeV<E< 200 MeV	1.74E-01	3.55E-02	1.44E+15	7.50E+14	8.34E+13	3.49E+13
200 MeV<E	3.49E-02	2.49E-01	4.28E+13	2.26E+13	2.30E+14	9.51E+13

Table 2: Fluence values in CeF_3 for a 24 GeV/c proton irradiation at the CERN PS and in the 2nd CeF_3 layer of a Shashlik CMS EE after 3000 fb^{-1} of collected data.

Energy interval	neutrons PS [cm^{-2}]	ch. had. PS [cm^{-2}]	CMS n η: 2.6-2.9 [cm^{-2}]	CMS n η: 2.2-2.6 [cm^{-2}]	CMS ch. had. η: 2.6-2.9 [cm^{-2}]	CMS ch.had. η: 2.2-2.6 [cm^{-2}]
E $<$ 0.5 MeV	1.89E-02	9.57E-06	4.64E+15	3.51E+15	1.25E+10	5.54E+09
0.5 MeV$<$E$<$ 20 MeV	5.30E-02	8.11E-05	1.93E+15	1.12E+15	1.20E+11	5.27E+10
20 MeV$<$E$<$ 200 MeV	1.72E-01	4.28E-02	1.37E+15	7.24E+14	7.95E+13	3.43E+13
200 MeV$<$E	5.48E-02	4.16E-01	4.75E+13	2.43E+13	3.08E+14	1.30E+14

Table 3: Fluence values needed for a 24 GeV/c proton irradiation of LYSO to reach the charged hadron fluence expected for the 2nd LYSO layer in the CMS EE for the given energy range in the interval $2.6 <| \eta |< 2.9$ after 3000 fb^{-1} of collected data.

Energy interval	neutrons [cm^{-2}]	ch. had. [cm^{-2}]
E $<$ 0.5 MeV	1.21E17	2.39E15
0.5 MeV$<$E$<$ 20 MeV	3.14E16	1.86E15
20 MeV$<$E$<$ 200 MeV	8.28E15	2.35E15
200 MeV$<$E	1.23E15	9.22E14

The fluences however vary depending on η and the Shashlik layer considered. This is illustrated in Fig. 4 for neutrons in three η intervals and in the first, second, seventh and last sampling layer of the calorimeter. In Fig. 4(a) one observes that, while the shape of the spectrum remaines unchaged for the different η bins, the overall level increases with increasing η. In Fig. 4(b) it is evident that in a given η bin, the fast neutron fluence is almost constant in depth, while the thermal and epithermal neutron fluence is higher in the first and last layer of the Shashlik calorimeter.

For a similar comparison, Fig. 5 depicts the charged hadron spectra, with the known maximum around 1 GeV. While the same observation applies as for neutrons in the η dependence, the fluences remain independent from the Shashlik layer considered.

To allow a simple scaling of damage measurements, the fluence values have been summarized for different intervals in energy. These values are given in the tables 1 and 2. To better grasp the correpondence between CMS running conditions and PS irradiations, ratios between the two situations are given in the following tables 3 and 4. It shall be reminded that the ionizing dose rate in proton irradiations is of the order of 1 kGy/h for a fluence of 10^{12} p/cm^{2}h [2].

It is important to point out, that the fluence in this note is a conservative estimate. The plots and values for the CMS scenario are derived with a BRIL approved FLUKA simulation (v.1.0.2.0 and v1.0.3.0). They are based on the nominal geometry (v1.0.0.0) describing the CMS geometry prior to LS1 [10]. Upstream to the Shashlik calorimeter, the current preshower acts as a placeholder for a possible future timing advice, the polyethylene moderator between preshower and endcap calorimeter is kept the same. The maximum pseudorapidity is $\eta = 2.9$ and the calorimeter consists of 15 layers of scintillator and 14 absorber layers, summing up to a radiation length of 25 X_0. Both scintillator options, CeF_3 and LYSO, are studied.
The baseline geometry for the CMS phase II technical proposal by BRIL (v3.7.0.0) includes a few modifications with respect to the previous geometry. The endcap calorimeter is extended up to $\eta = 3.0$. Upstream to the endcap calorimeter, the preshower is replaced by a Boron polyethylene absorber, which not only moderates neutrons, but also absorbs the thermalized ones. For the Shashlik calorimeter option (v3.7.1.0), the lead tungstate crystals in

Table 4: In a 24 GeV/c proton irradiation of LYSO up to 9.22×10^{14} cm^{-2}, fluence fractions in different energy ranges with respect to the 2nd LYSO layer in the CMS EE in the interval $2.6 <| \eta |< 2.9$ after 3000 fb^{-1} of collected data.

Energy interval	neutrons [cm^{-2}]	ch. had. [cm^{-2}]
E $<$ 0.5 MeV	0.8%	39%
0.5 MeV$<$E$<$ 20 MeV	2.9%	50%
20 MeV$<$E$<$ 200 MeV	11.1%	39%
200 MeV$<$E	75.2%	100%

the endcap region are replaced by an averaged material accounting for the LYSO/W option. Further details to this simulation can be found in the technical proposal for the phase II CMS detector.

4 Neutron spectrum characteristics

Fig. 4(b) shows typical neutron spectra. In the region of low energy neutrons, the number and width of the bins is given by the thermal neutron cross section library in FLUKA. Thermal neutrons carry an energy up to a few eV with the thermal peak being between 10^{-11} GeV and 10^{-10} GeV. This region is followed by a resolved resonance region, where the neutrons are absorbed via inelastic scattering. These resonances depend on the elements in the materials as can be seen in Fig. 2, where the neutron energy spectra show a different behaviour depending on the scintillator materials. The intermediate energy region depicts the caracteristic evaporation peak around 1-5 MeV, followed by the knock-out peak around 100 MeV.
The distributions for different layers in Fig. 4(b) show a lower fluence for low energy neutrons in the middle of the calorimeter (7th layer). As expected, the resolved resonance region is here more distinct. An explanation for the different magnitude could be that the Shashlik calorimeter produces many neutrons at intermediate energies, which might escape. In the surrounding materials, these neutrons can be thermalized. Thermal neutrons are only captured by light elements or elements with a large thermal neutron absorption cross section. A previous study in Ref. [10] showed that the incoming thermal neutron fluence at the surface of the first scintillator layer is considerably higher than the outgoing fluence from the Shashlik calorimeter. This behaviour can be observed for CeF_3 and LYSO.

5 On damage to crystals depending on particle energy

Concerning neutron damage to Lead Tungstate, the studies published in Refs. [2, 4] have demonstrated, how the hadron-specific damage scales with the density of "stars" using FLUKA simulations. Neutrons with energies below 20 MeV do not produce any stars, and can thus be neglected for the evaluation of the expected damage [2]. A discussion is found in an earlier study [11], about the hadron-specific damage caused by neutrons in CeF_3 depending on the energy. The conclusion is, that the effect of thermal and epithermal neutrons is negligible, and that the radiation-induced aptical absorption is only caused by fast neutrons. The significant neutron fluence should thus be of the order of a few 10^{14} n/cm^2. Similarly, for LYSO. The absorption of thermal neutrons create unstable isotopes. The impact of this decay is studied for CMS running conditions in Ref. [10]. It is shown therein, that the ionizing dose rate due to the decay products is at a constant 1% level of the one caused by prompt particles.

Conclusions

This note gives a simple means to scale between proton irradiations of scintillating crystals to CMS running conditions. Scaling factors for the neutron fluence depend on the energy bin considered, while for the charged hadron fluence an overall scaling factor can be determined.

Acknowledgements

We are grateful to Francesca Cavallari and to the members of the BRIL radiation simulation group for their valuable input to this study.

References

[1] F. Nessi-Tedaldi, *"Studies of the effect of charged hadrons on lead tungstate crystals"*, J. Physics: Conf. Series 160 (2009) 012013.

[2] M. Huhtinen, P. Lecomte, D. Luckey, F. Nessi-Tedaldi, F. Pauss, *"High-energy proton induced damage in $PbWO_4$ calorimeter crystals"*, Nucl. Instr. and Meth. A 545 (2005) 63-87.

[3] P. Lecomte, D. Luckey, F. Nessi-Tedaldi, F. Pauss, *"High-energy proton damage study of scintillation light output from $PbWO_4$ calorimeter crystals"*, Nucl. Instr. and Meth. A 564 (2006) 164-168.

[4] D. Renker, P. Lecomte, D. Luckey, F. Nessi-Tedaldi, F. Pauss, *"Comparison between high-energy proton and charged pion induced damage in $PbWO_4$ calorimeter crystals"*, Nucl. Instr. and Meth. A 587 (2008) 266 - 271.

[5] A. S. Iljinov et al, *"Comparison of fission of heavy nuclei induced by different probes"*, Phys. Rev. C 39 (1989) 1420-1424.

[6] G. Dissertori, P. Lecomte, D. Luckey, F. Nessi-Tedaldi, F. Pauss, Ch. Urscheler, Th. Otto, S. Roesler, *"A study of high-energy proton induced damage in Cerium Fluoride in comparison with measurements in Lead Tungstate calorimeter crystals"*, Nucl. Instr. and Meth. A 622 (2010) 41-48.

[7] G. Dissertori, D. Luckey, F. Nessi-Tedaldi, F. Pauss, M. Quittnat, R. Wallny, M. Glaser, *"Results on damage induced by high-energy protons in LYSO calorimeter crystals"*, Nucl. Instr. and Meth. A 745 (2014) 1-6.

[8] F. Nessi-Tedaldi, '*Charged hadron damage in crystals"*, in CMS ECAL crystal detector performance group meeting, February 27th, 2008 (Cern, Geneva, Switzerland, 2008), http://indico.cern.ch/conferenceDisplay.py?confId=29683

[9] The CMS ECAL group, P. Adzic et al., *"Radiation hardness qualication of $PbWO_4$ scintillation crystals for the CMS Electromagnetic Calorimeter"*, 2010 JINST 5 P03010.

[10] M. Quittnat (CMS collaboration), *"FLUKA studies of hadron-irradiated scintillating crystals for calorimetry at the High-Luminosity LHC"*, CMS Conference Report CMS CR -2014/067.

[11] R. Chipaux, J.-L. Faure, P. Rebourgeard, *"Behaviour of CeF_3 scintillator in an LHC-like environment*, Nucl. Instr. and Meth. A 345 (1994) 440-444.